Supplementary materials:

RRCGAN: Unsupervised Compression of Radiometric Resolution of Remote Sensing Images Using Contrastive Learning

Abstract: The majority of current remote sensing images possess high-radiometric resolution exceeding 10 bits. Precisely compressing this radiometric resolution to 8 bits is crucial for visualization and subsequent deep learning tasks. Previously, radiometric resolution compression required extensive parameter adjustments of traditional tone mapping operators. Deep learning is gradually replacing this high manual dependency method. However, existing deep learning tone mapping techniques are primarily designed for natural scene images captured by digital cameras, making direct application to remote sensing images challenging. This limitation stems from disparities in data formats and the complexity of semantic representation in remote sensing images. Moreover, the block prediction inherent in deep learning models often results in tiling artifacts post-splicing, failing to satisfy the scale dependency of remote sensing images. To tackle these challenges, we propose leveraging contrastive learning methods to compress the radiometric resolution of remote sensing images. Given the rich detail information and complex spatial distribution of objects in remote sensing images, we develop a CNN-Transformer hybrid generator capable of capturing both local details and long-range dependencies. Building upon this, we introduce non-local self-similarity contrastive loss and histogram similarity loss to enhance feature expression and regulate image color distribution. Additionally, we present a post-processing technique based on hybrid histogram matching to enhance image quality and seamlessly generate whole-scene images. Through experiments and comparisons on our dataset, our method demonstrates superior performance. The dataset and code can be obtained online in this link https://github.com/ZzzTD/RRCGAN.

Keyword: High Radiometric Resolution Remote Sensing Images，Radiometric Resolution Compression，Image-to-Image Translation，Contrastive Learning，Generative Adversarial Networks

We have provided more local demonstrations of the methods and post-processing methods in this paper. Fig. S1. to Fig. S4. show the results of the JL1 dataset, Fig. S5 to Fig. S8. show the results of the GF7 dataset and Fig. S9 to Fig. S12. show the results of the GF2 dataset. It can be seen that when RRCGAN results have deficiencies in contrast, brightness, etc., the post-processing method can effectively improve RRCGAN-HHM.

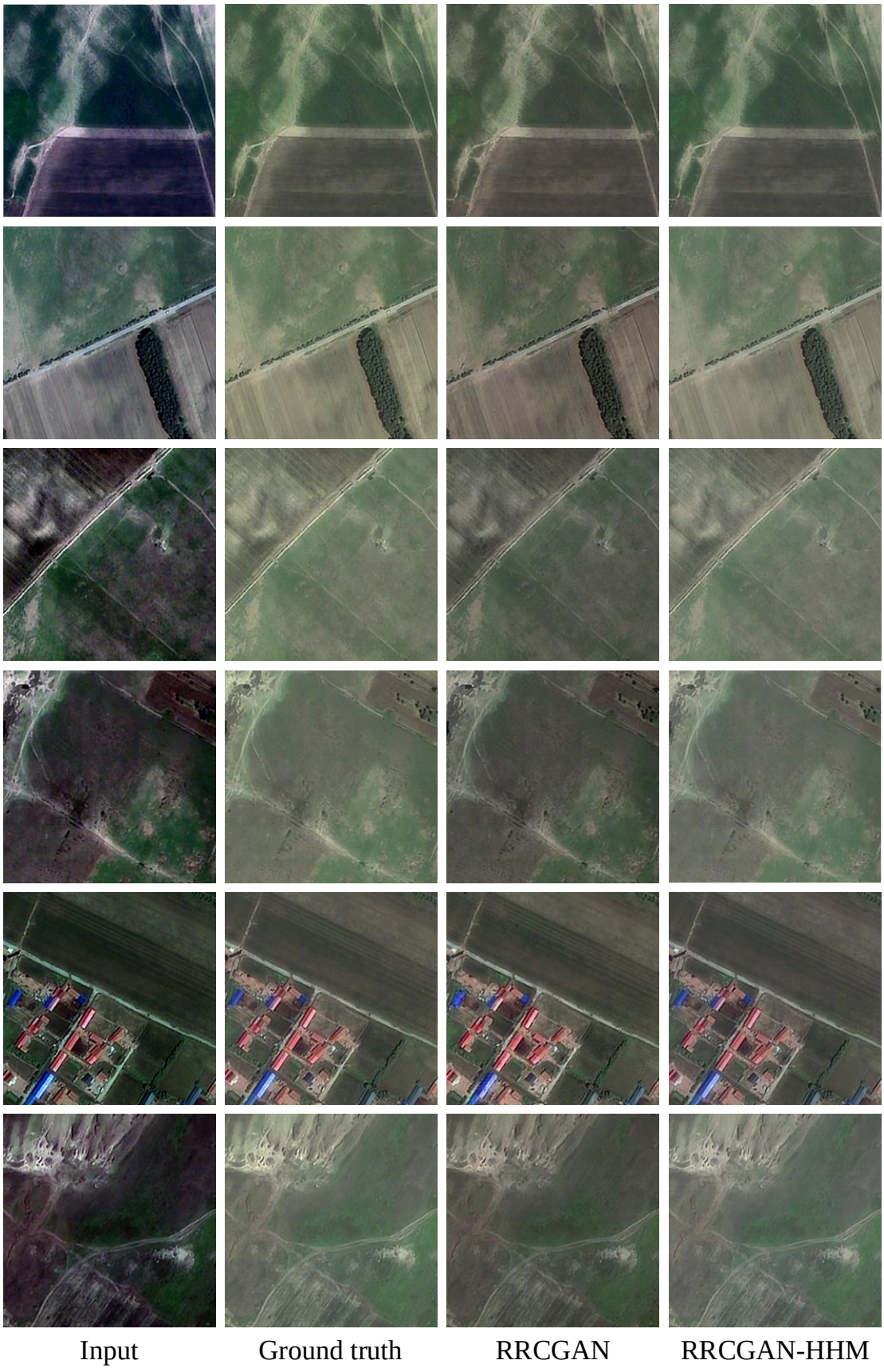

Fig. S1. JL1 result1. From left to right: is the 16bit image opened by ENVI, Ground truth, our proposed RRCGAN, and the post-processing method RRCGAN-HHM. Zoom in for clarity.

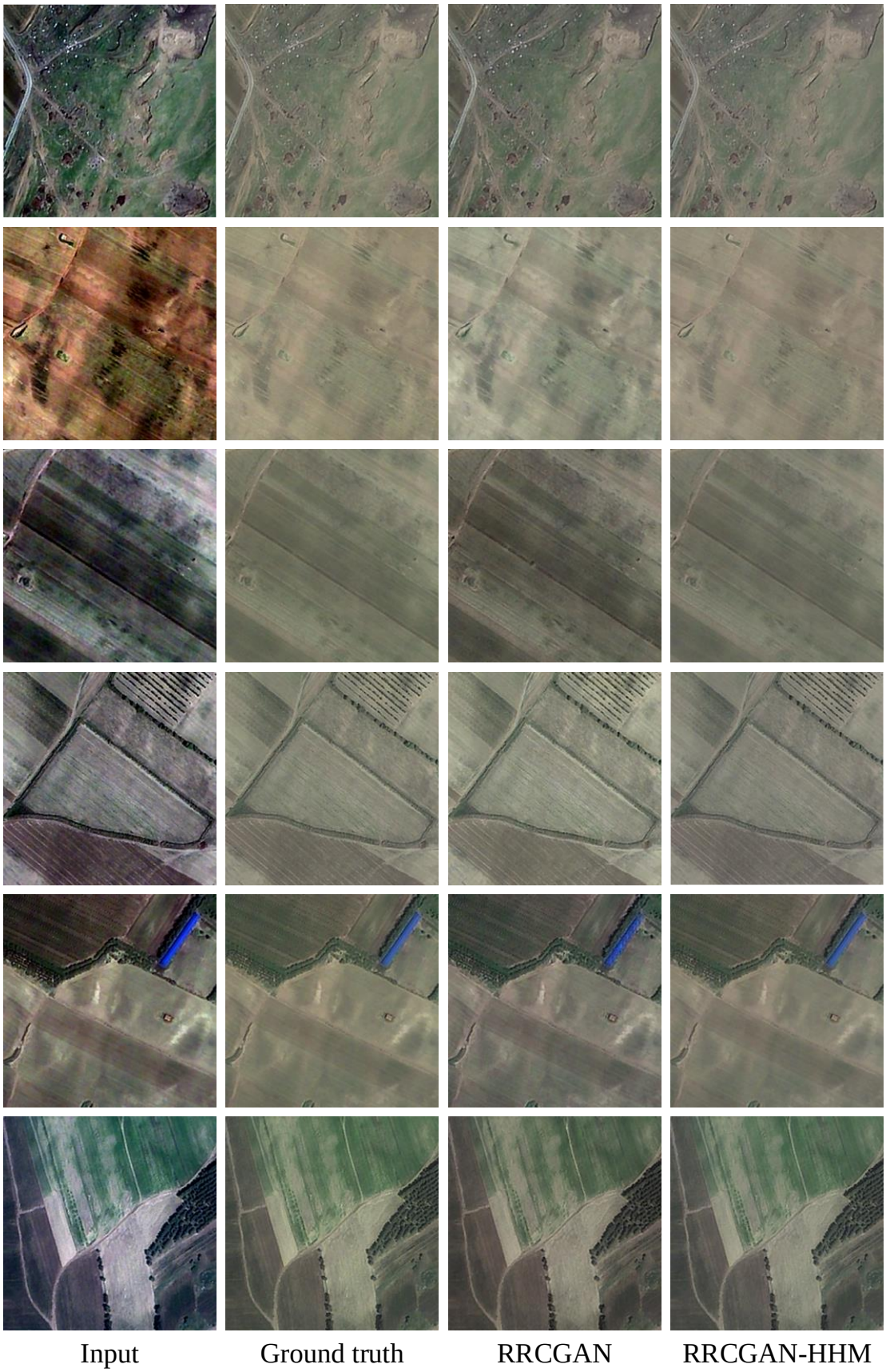

Fig. S2. JL1 result2. From left to right: is the 16bit image opened by ENVI, Ground truth, our proposed RRCGAN, and the post-processing method RRCGAN-HHM. Zoom in for clarity.

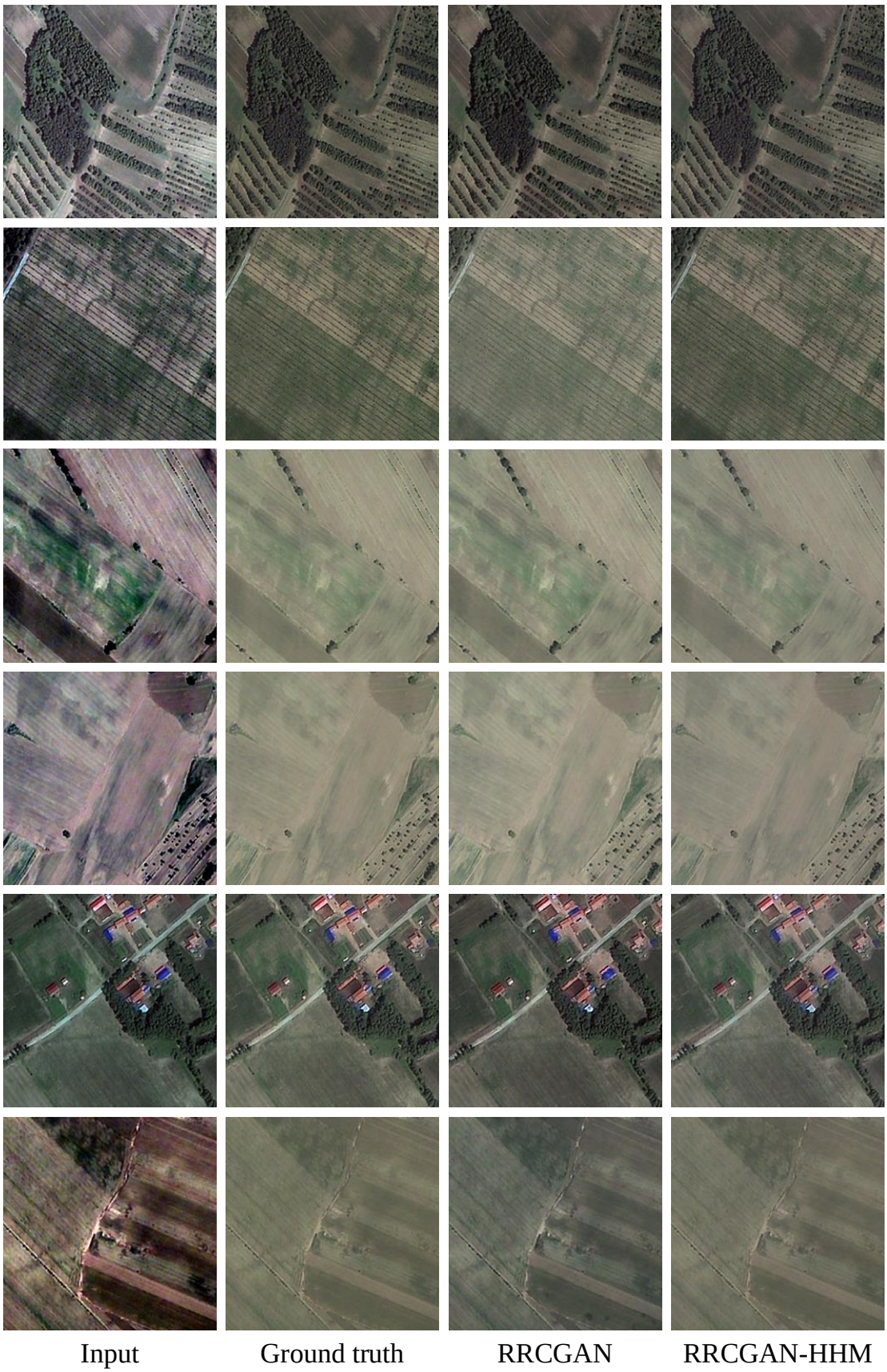

Fig. S3. JL1 result3. From left to right: is the 16bit image opened by ENVI, Ground truth, our proposed RRCGAN, and the post-processing method RRCGAN-HHM. Zoom in for clarity.

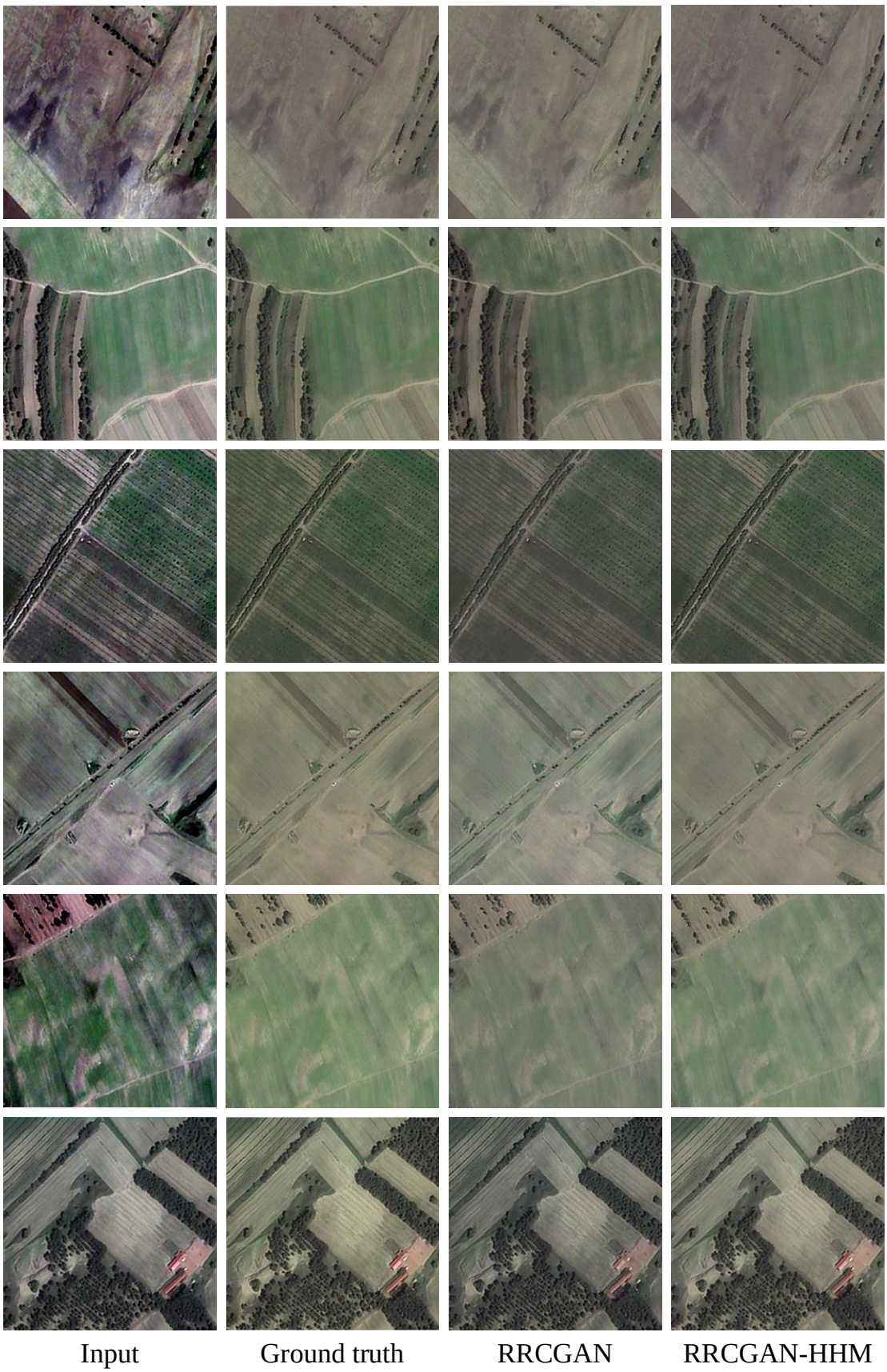

Fig. S4. JL1 result4. From left to right: is the 16bit image opened by ENVI, Ground truth, our proposed RRCGAN, and the post-processing method RRCGAN-HHM. Zoom in for clarity.

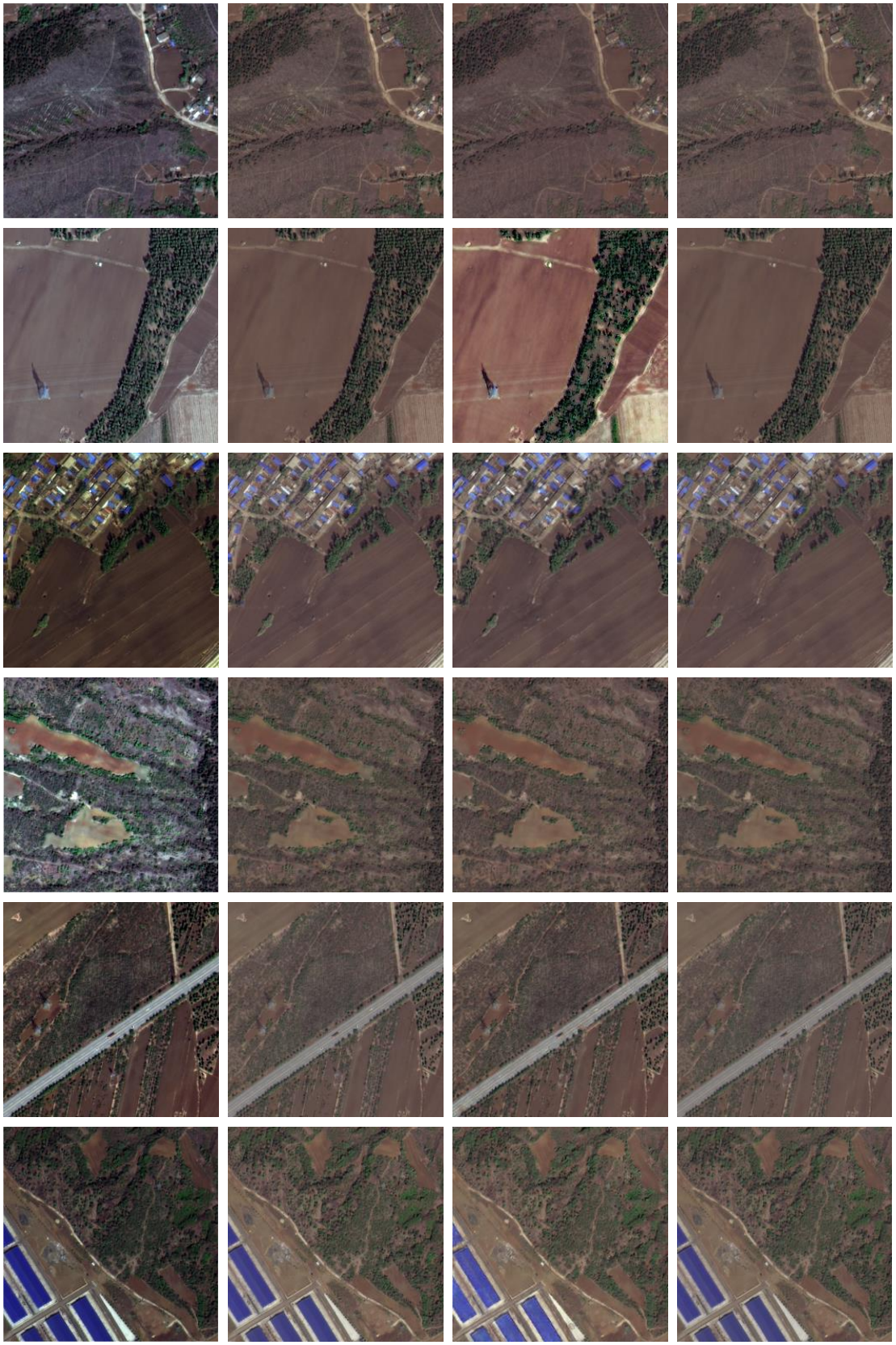

Fig. S5. GF7 result1. From left to right: is the 16bit image opened by ENVI, Ground truth, our proposed RRCGAN, and the post-processing method RRCGAN-HHM. Zoom in for clarity.

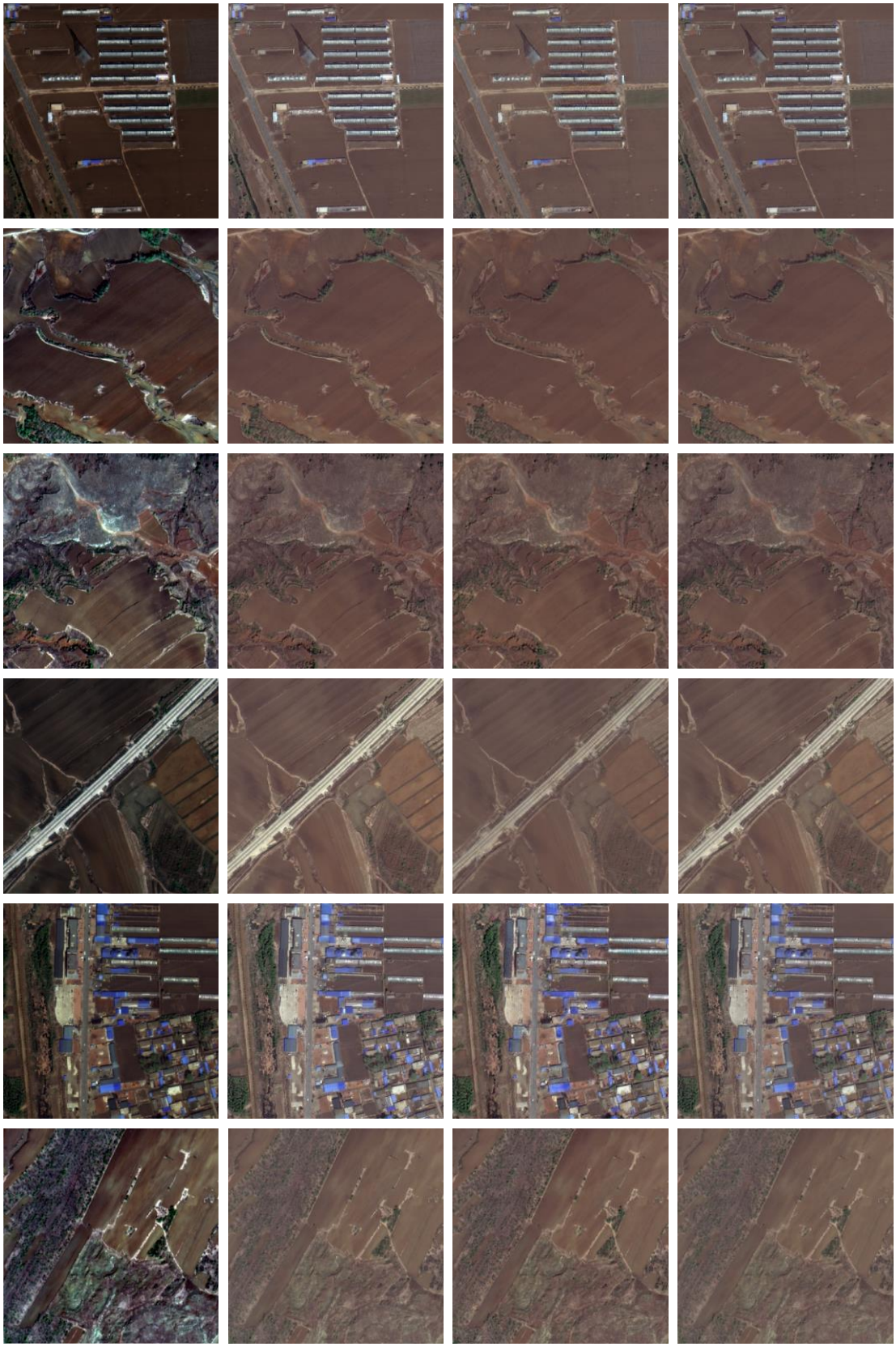

Fig. S6. GF7 result2. From left to right: is the 16bit image opened by ENVI, Ground truth, our proposed RRCGAN, and the post-processing method RRCGAN-HHM. Zoom in for clarity.

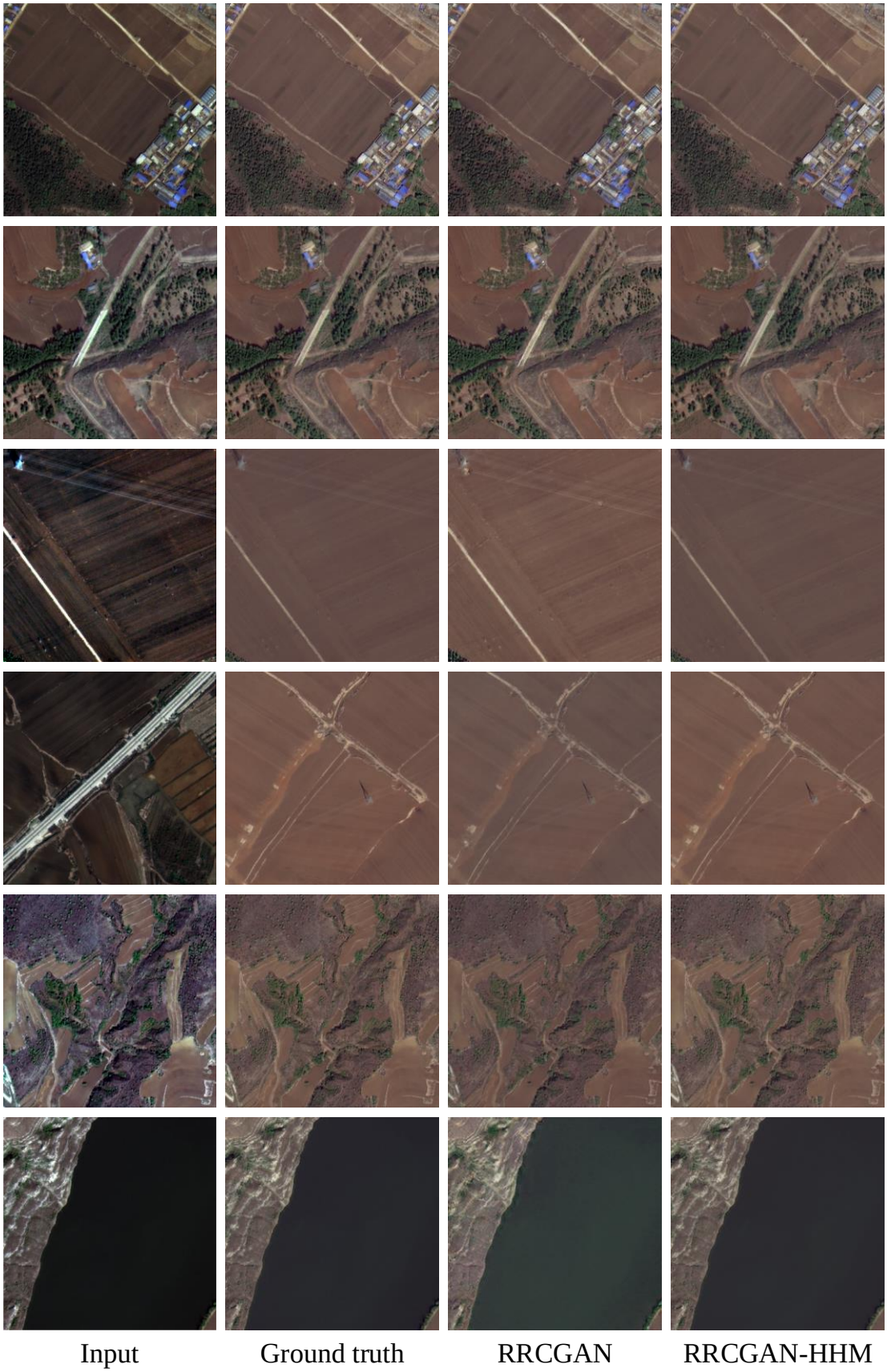

Fig. S7. GF7 result3. From left to right: is the 16bit image opened by ENVI, Ground truth, our proposed RRCGAN, and the post-processing method RRCGAN-HHM. Zoom in for clarity.

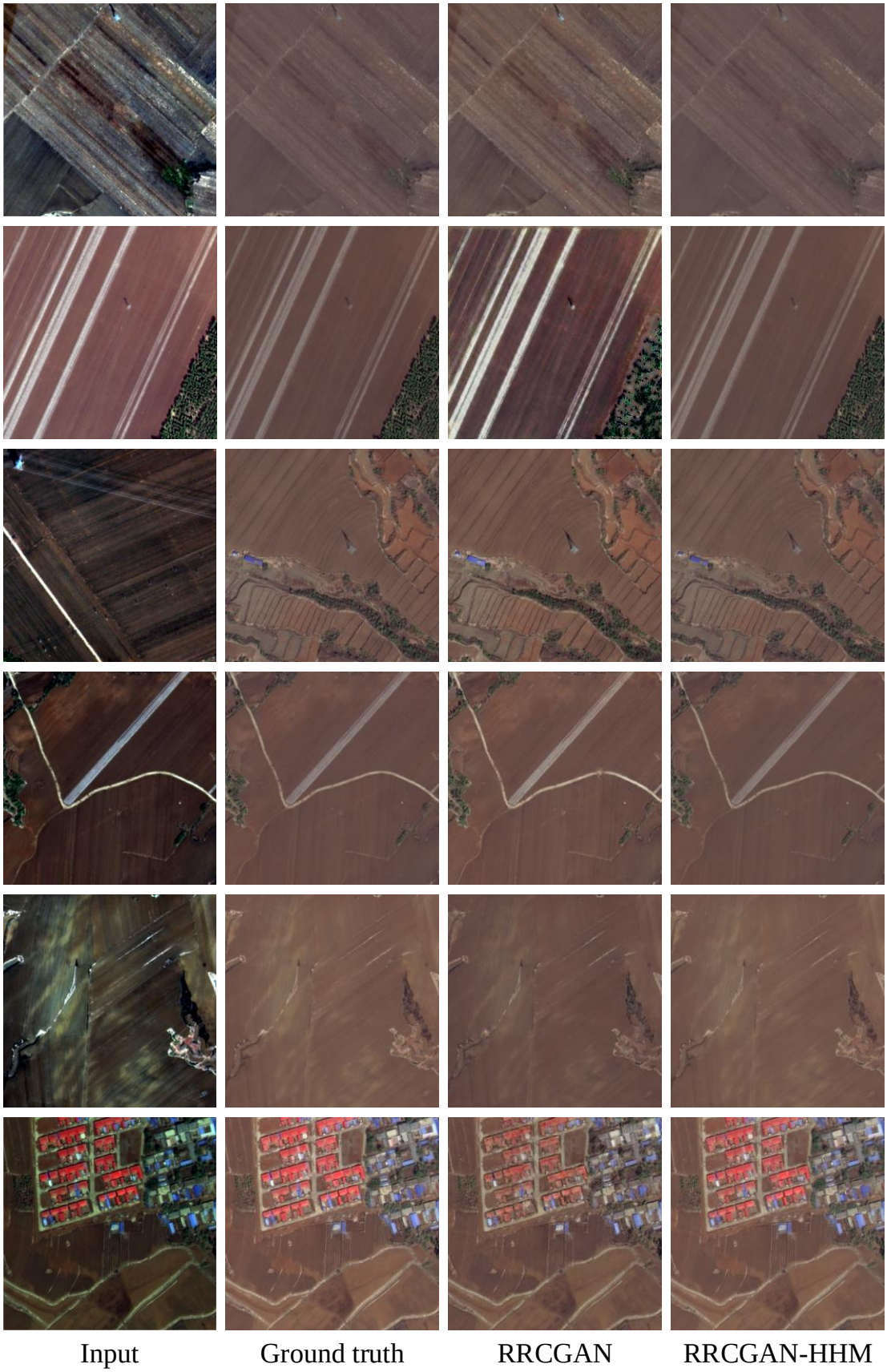

Fig. S8. GF7 result4. From left to right: is the 16bit image opened by ENVI, Ground truth, our proposed RRCGAN, and the post-processing method RRCGAN-HHM. Zoom in for clarity.

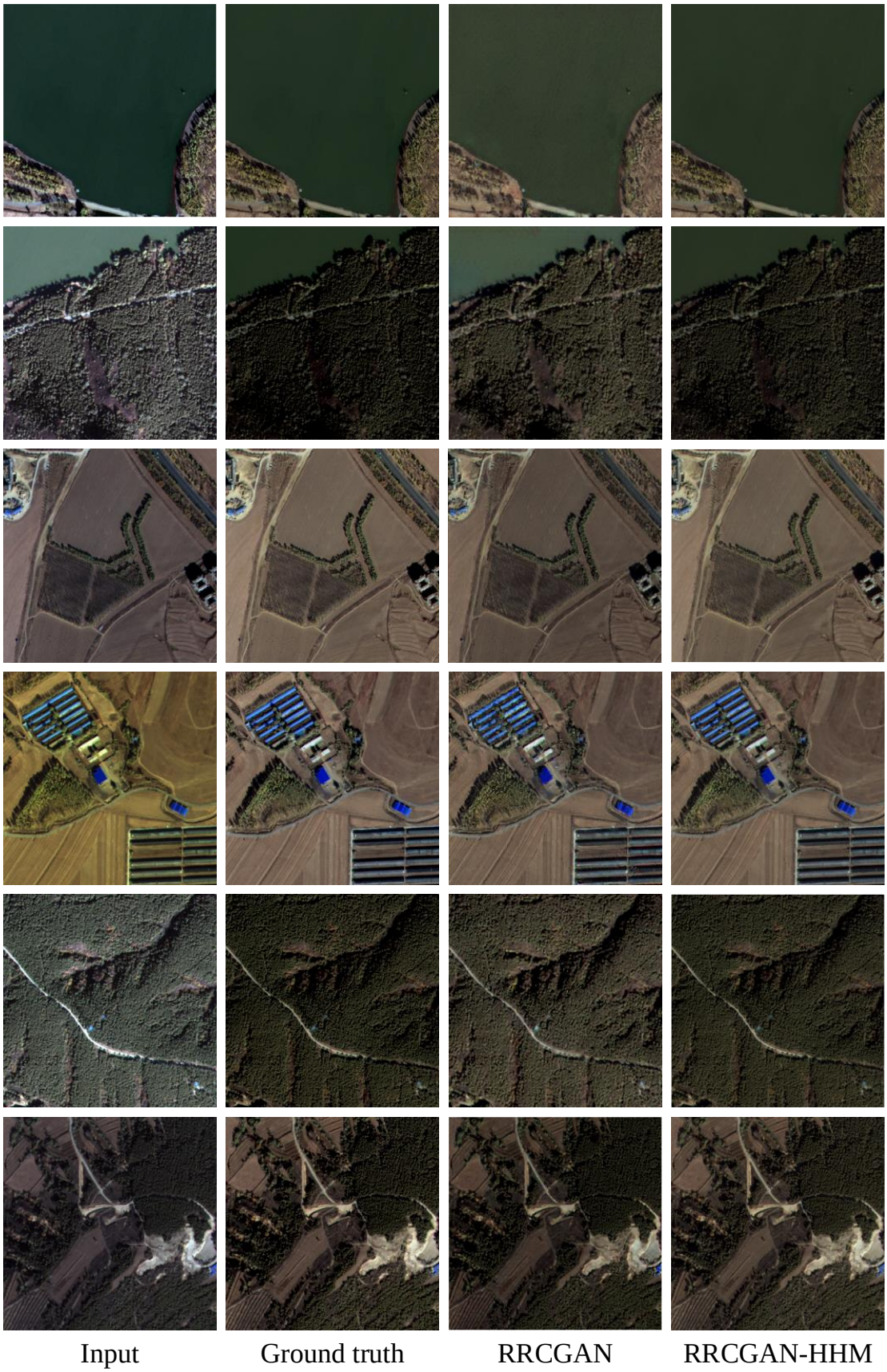

Fig. S9. GF2 result4. From left to right: is the 16bit image opened by ENVI, Ground truth, our proposed RRCGAN, and the post-processing method RRCGAN-HHM. Zoom in for clarity.

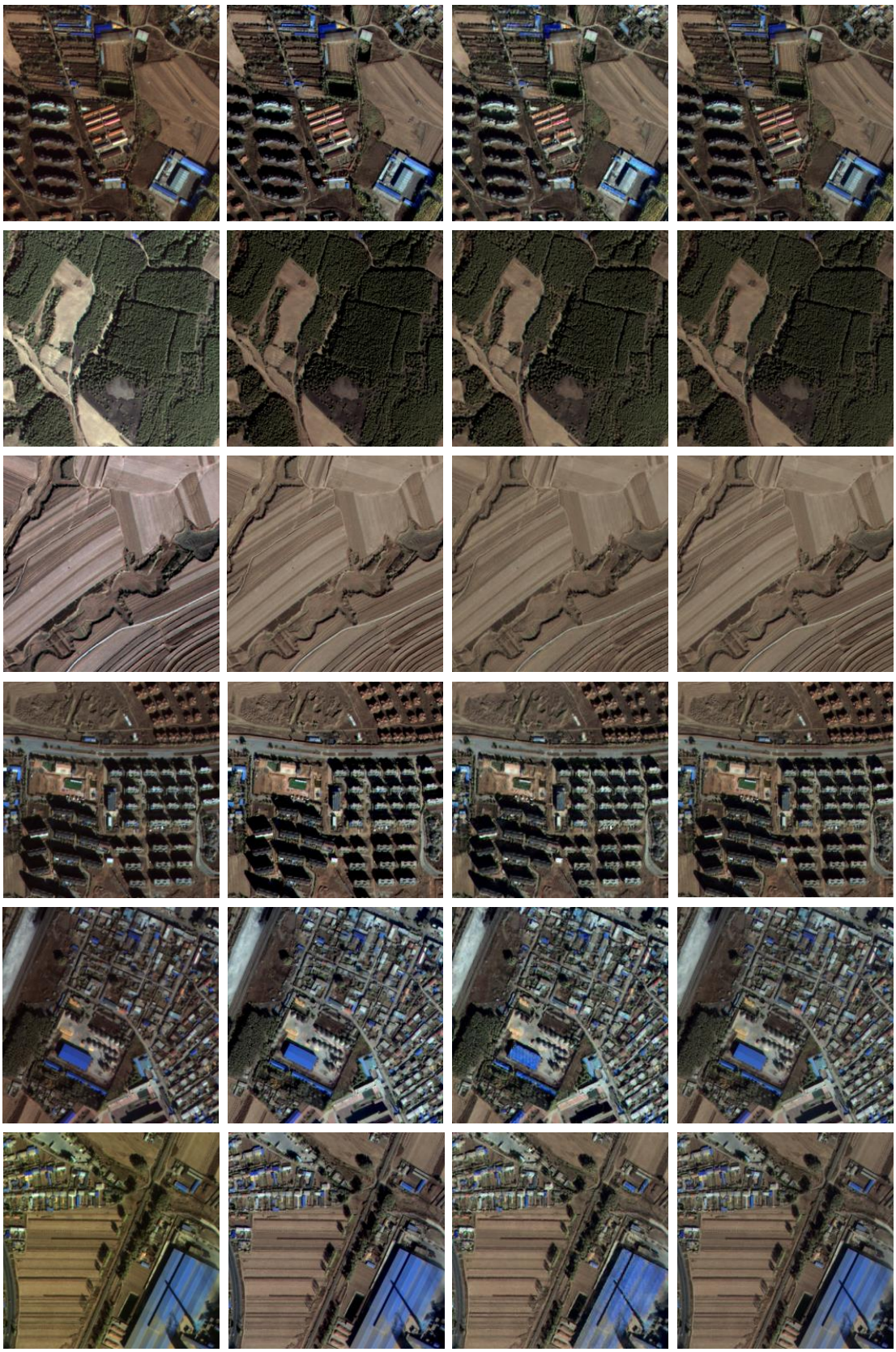

Fig. S10. GF2 result4. From left to right: is the 16bit image opened by ENVI, Ground truth, our proposed RRCGAN, and the post-processing method RRCGAN-HHM. Zoom in for clarity.

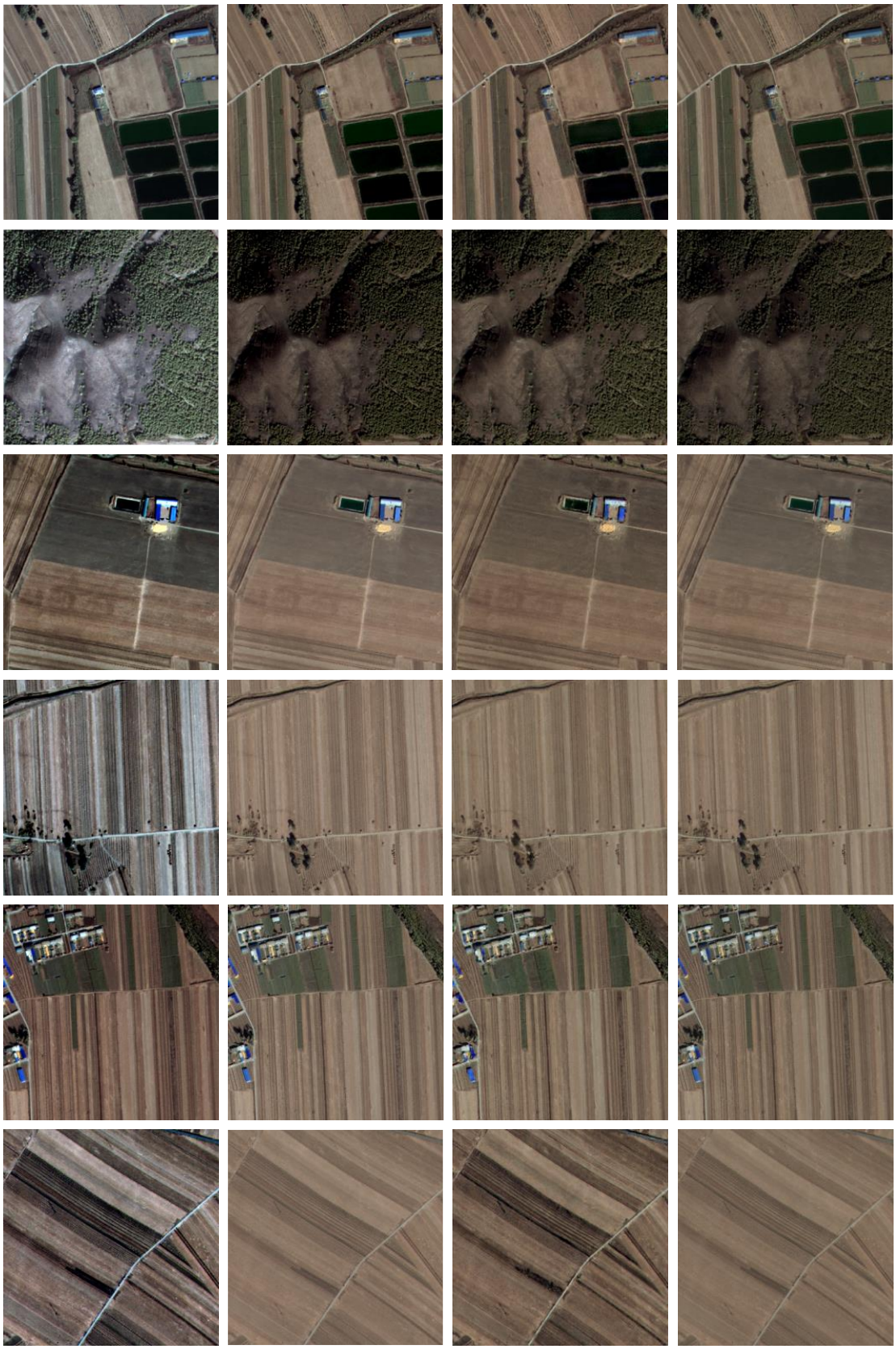

Fig. S11. GF2 result4. From left to right: is the 16bit image opened by ENVI, Ground truth, our proposed RRCGAN, and the post-processing method RRCGAN-HHM. Zoom in for clarity.

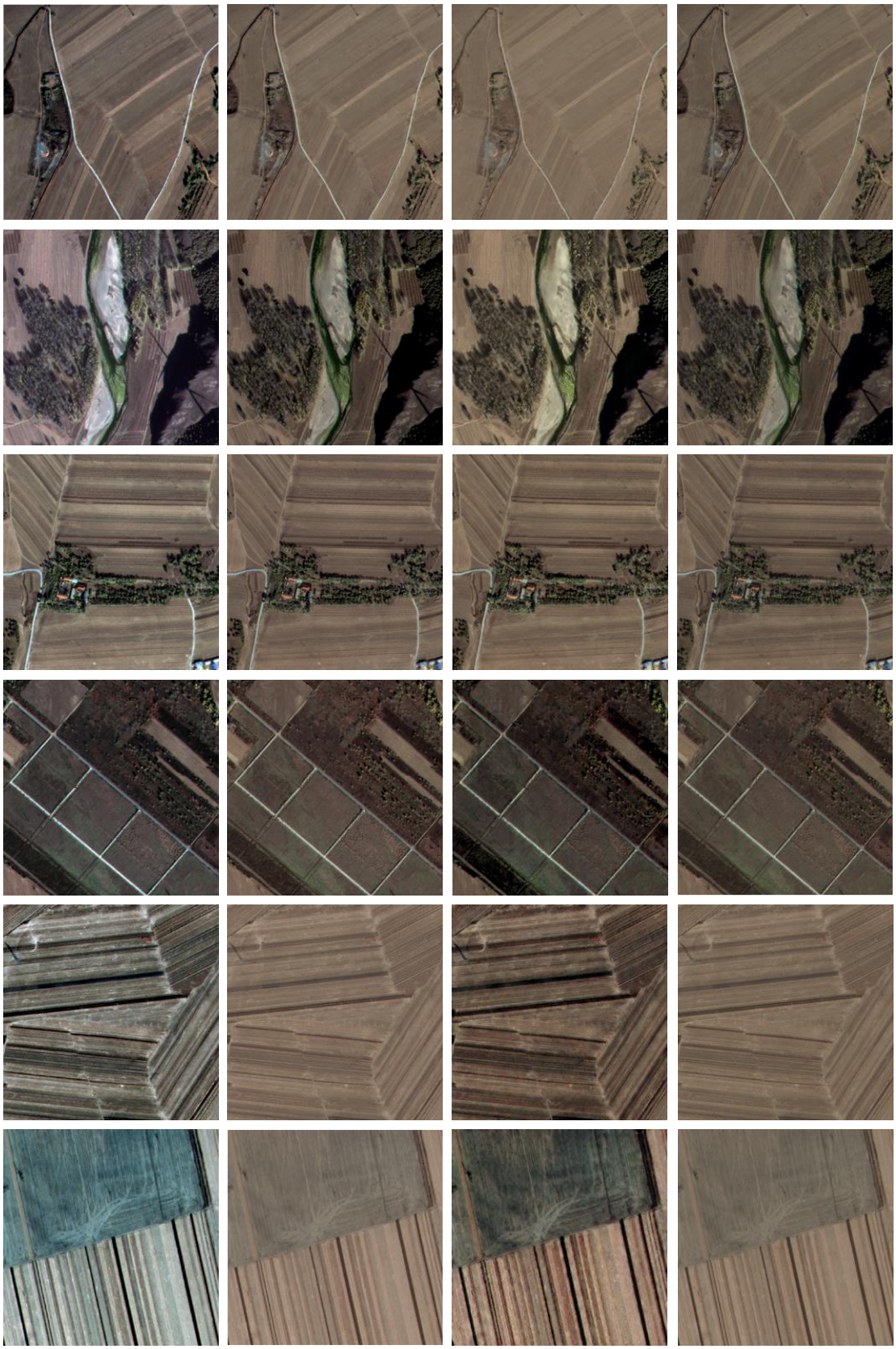

Fig. S12. GF2 result4. From left to right: is the 16bit image opened by ENVI, Ground truth, our proposed RRCGAN, and the post-processing method RRCGAN-HHM. Zoom in for clarity.